# The *N*-linked Oligosaccharides of the β-Subunit of Rabbit Gastric H,K-ATPase: Site Localization and Identification of Novel Structures†

Kamala Tyagarajan,‡ Peter H. Lipniunas,§,|| R. Reid Townsend,||,⊥ and John G. Forte*,‡

*Department of Molecular and Cell Biology, University of California, Berkeley, California 94720-3200, and Department of Pharmaceutical Chemistry, University of California, San Francisco, California 94143-0446*

*Received March 17, 1997; Revised Manuscript Received June 5, 1997*⊗

ABSTRACT: The gastric H,K-ATPase is responsible for acid secretion by parietal cells. Its β-subunit is a glycoprotein which is exposed to the harsh, acidic environment of the stomach. The location and structural features of the *N*-linked oligosaccharides were determined using matrix-assisted laser desorption ionization mass spectrometry (MALDI/MS) (in conjunction with mass composition analysis and exoglycosidase digestions), Edman degradation, and monosaccharide composition analysis. All seven *N*-linked sequons at positions 99, 103, 130, 146, 161, 193, and 222 were fully glycosylated. An unusual restricted array of oligosaccharides was observed at individual Asn residues. $Asn^{99}$ was modified exclusively with oligomannosidic-type structures ($Man_6GlcNAc_2$-$Man_8GlcNAc_2$). $Asn^{193}$ contained both oligomannosidic ($Man_5GlcNAc_2$-$Man_8GlcNAc_2$) and lactosamine-type structures, indicating significant "leakiness" in the pathway which converts oligomannose to lactosamine-type at a single glycosylation site. MALDI/MS with collision-induced dissociation was required to demonstrate that sequons separated by a single residue ($^{99}$Asn-Ile-Ser-Asp-Asn-Arg-Thr$^{105}$) were modified with only oligomannose and lactosamine structures, respectively. Analysis of the total oligosaccharide pool using MALDI/MS and exoglycosidase analysis revealed 24 lactosamine species (bi-, tri-, and tetraantennary structures), with all branches terminated in α-linked Gal residues, most possessing a single Fuc residue. Nine novel oligosaccharides contained multiple α-linked Gal residues per branch. Bi- and triantennary structures, with and without lactosamine repeats, were observed at $Asn^{146}$ and $Asn^{161}$. Tetraantennary structures with lactosamine repeats were found only at $Asn^{130}$, and this site also contained most of the structures with multiple α-linked Gal residues per branch.

The gastric H,K-ATPase is the proton-translocating ATPase which is found in parietal cells and is responsible for acid secretion by the stomach. The protein is a heterodimer consisting of a catalytic α-subunit and a β-subunit, which is also essential for holoenzyme function (*1*, *2*). The β-subunit of the H,K-ATPase (gastric β-subunit) consists of a polypeptide chain of 32 kDa, with an apparent molecular weight on SDS−PAGE gels of 60−80 kDa due to modification by *N*-linked oligosaccharides. The amino acid sequence of the gastric β-subunit of most species examined reveals the presence of seven potential *N*-linked sites of glycosylation (*3*−*5*); the pig β-subunit is an exception in which only $Asn^{103}$ is not conserved (*6*). A homologous feature of the gastric β-subunits from all species is the presence of nine cysteine residues, of which six are located in the extracellular domain and are present in the oxidized form (*1*). Interestingly, two of the oxidized cysteines, $Cys^{131}$ and $Cys^{162}$, occur within the glycosylation sequons containing $Asn^{130}$ and $Asn^{161}$. Two potential glycosylation sequons containing $Asn^{99}$ and $Asn^{103}$ are separated by only one amino acid residue, and it would be of interest to determine whether they are glycosylated and to determine the structure of glycans at each sequon.

The β-subunit is essential for the function of the holotransporter (*1*, *2*). The role of the oligosaccharides in enzyme function is not clear; however, it has been suggested that the oligosaccharides of the gastric β-subunit may play a role in the trafficking (*7*) and survival of the enzyme in the harsh acidic environment of the stomach (*8*). The nature of the oligosaccharides on the gastric β-subunit may also be important, since it has been demonstrated that they contain no sialic acid in all species examined (*9*−*11*). We recently suggested that a part of the adaptation of the gastric β-subunit to the acidic environment of the stomach is through providing acid-stable terminal residues on the oligosaccharides (*12*). The gastric β-subunit from several animal species has been shown to be recognized by parietal cell autoantibodies associated with chronic atrophic gastritis in humans (*13*). The reactivity of these autoantibodies involves the carbohydrate moiety; however, there also appears to be a contribution from the peptide moiety (*14*). Determination of the glycosylated sequons and of the site-specific distribution of oligosaccharides on the gastric β-subunit is required to understand the role of carbohydrates in H,K-ATPase function and trafficking and may provide insights to the mechanism of autoimmune gastritis.

† This work was supported in part by NIH Grant DK 38972, the Biomedical Research Technology Program of the National Center for Research Resources (NIH NCRR BRTP 01614 and RR08282), and NSF DIR 8700766.

* To whom correspondence and reprint requests should be sent. Tel: (510) 642-1544. FAX: (510) 643-6791. E-mail: jforte@uclink2.berkeley.edu.

‡ UC Berkeley.

§ UCSF.

|| Current address: Astra Draco AB, P.O. Box 34 S-22100, Lund, Sweden.

⊥ To whom reprint requests may also be sent at UCSF. Tel: (415) 476-5189. FAX: (510) 476-0688. E-mail: rrtown@itsa.ucsf.edu.

⊗ Abstract published in *Advance ACS Abstracts,* August 1, 1997.

S0006-2960(97)00612-0 CCC: $14.00 

We recently reported the characterization of oligosaccharides from the rabbit gastric β-subunit, demonstrating that the oligosaccharides are a mixture of oligomannosidic and lactosamine-type structures. Interestingly, all branches of the lactosamine-type oligosaccharides were terminated in GalαGalβ residues (*12*). In the present study, our aim was to identify which sequons on the gastric β-subunit are glycosylated and to determine the distribution of oligosaccharides at each individual site. Our studies here demonstrate that all seven sequons on the rabbit gastric β-subunit are fully glycosylated. Further, there was a intriguing site-specific distribution of oligosaccharides: two "close-proximity" sequons separated by only one amino acid had different classes of oligosaccharides, with oligomannosidic-type at $Asn^{99}$ and lactosamine-type at $Asn^{103}$. Two sites, $Asn^{99}$ and $Asn^{193}$, were predominantly modified with oligomannosidic glycans, while the other five sites were glycosylated with mono-fucosylated lactosamine-type oligosaccharides with GalαGal termini. Novel linear polylactosmine structures with more than one α-Gal residue per branch were found at Asn residues 130, 146, and 161.

## MATERIALS AND METHODS

*Materials*. Trypsin, sodium iodoacetate, dithiothreitol, sodium iodoacetate, adrenocorticotropic hormone fragment (18−39), bovine insulin oxidized B chain, human recombinant insulin, ubiquitin, and egg white lysozyme were purchased from Sigma (St. Louis, MO). Chicken liver fucosidase and coffee bean α-galactosidase were from Oxford Glycosystems (Abingdon, U.K.). HPLC grade water, acetonitrile, ammonium bicarbonate, sodium hydroxide (50% solution), sodium acetate, and calcium chloride were purchased from Fisher (Pittsburgh, PA). HPLC grade TFA and guanidine hydrochloride and trifluoroacetic acid were from Pierce (Rockford, IL). Dialysis membranes were purchased from GIBCO, Life Technologies (Gaithersburg, MD). PNGase F[1] (glycerol free) was provided by Dr. Tony Tarentino, New York, Department of Health, Albany, NY. Endoglycosidase H and β-galactosidase were purchased from Boehringer Mannheim (Indianapolis, IN). Matrices for MALDI/MS [2,5-dihydroxybenzoic acid (DHB) and α-cyano-4-hydroxycinnamic acid] were from Hewlett Packard (Palo Alto, CA). The low molecular weight calibration set was obtained from Bio-Rad (Richmond, CA).

*Purification of the Gastric β-Subunit*. H,K-ATPase-enriched gastric microsomes were isolated from rabbit stomach as previously described (*15*). Crude microsomes were harvested from homogenized mucosa of unstimulated rabbit stomach ($H_2$ receptor-blocked) as the membrane pellet sedimenting between 10 min at 13000*g* and 1 h at 100000*g*. The pellet was resuspended in 10% (w/v) sucrose, brought to 40% sucrose (9 mL), and overlaid with successive layers of 30% sucrose (11 mL) and 10% sucrose (16 mL) [300 mM sucrose, 5 mM tris(hydroxymethyl)aminomethane (Tris), and 0.2 mM EDTA, pH 7.4] in a 37 mL tube. After centrifugation at 80000*g* for 4 h, the purified gastric microsomes were collected from the interface between 10% and 30% sucrose and stored at 4 °C until use. The β-subunit was purified from H,K-ATPase-enriched rabbit microsomes as described previously (*16*). The binding and nonbinding fractions were resuspended in 10 mM sodium phosphate pH 7.0, quantitated by Bradford assays, and the purity was checked by SDS−PAGE gels followed by Coomassie Blue staining.

*Tryptic Digestion of the β-Subunit*. A 30 μg amount of purified gastric β-subunit was reduced with DTT (40 mM) in Gu-HCl (6 M), Tris-HCl (200 mM, pH 8.0), for 1.5 h at 60 °C. The protein was next alkylated with sodium iodoacetate (125 mM in 0.2 M Tris, pH 8.0) for 1.5 h under argon. The solution was dialyzed in a BRL microdialyzer unit for 21 h against $NH_4HCO_3$ (50 mM, pH 7.5). The solution was dried in a SpeedVac concentrator (Savant model SVC 100) and then resuspended in 150 μL of $NH_4HC0_3$ (100 mM, pH 8.0) buffer containing $CaCl_2$ (1 mM). Trypsin (2.5 μg) was added, and the reaction was allowed to proceed for 22 h at 37 °C with a second aliquot being added after 4 h (1:15 ratio of trypsin to β-subunit). The digest was boiled in water for 10 min.

*Reversed-Phase HPLC Separation of the Tryptic Digest*. The entire digest (∼1 nmol) was separated on an Aquapore OD-300 (1 × 250 mm) C18 reverse phase column (Applied Biosystems Inc.) using a Michrom UMA Model 600 HPLC system with eluant monitoring at 214 nm. The first 5 min of the gradient was isocratic at 5% eluant B (98% $CH_3CN$, 0.1% TFA) and 95% eluant A (2% $CH_3CN$, 0.1% TFA). This was followed by a linear gradient of 5−15% B in 15 min, 15−50% B at 75 min, and 50−75% B at 90 min. The flow rate was 50 μL/min. Forty individual fractions were collected and stored at −20 °C.

*Oligosaccharide Release and Labeling*. The *N*-linked oligosaccharides were released from ∼8 nmol (275 μg of protein) of purified β-subunit of the rabbit H,K-ATPase by incubation at 37 °C for 18 h with 100 milliunits of PNGase F (glycerol-free) in a sodium phosphate buffer (10 mM, pH 7.5) in a final volume of 280 μl. One milliunit of PNGase F activity is defined as the amount of enzyme required to hydrolyze 1 nmol of a pentaglycopeptide from bovine fetuin (*17*).

Reducing oligosaccharides were coupled to 2-AB as previously described (*18*). Briefly, 12 μL (345 pmol of protein) of β-subunit PNGase F digest was dried. The digest was dissolved in 5 μL of a solution of 2-AB (0.35 M) in dimethyl sulfoxide/glacial acetic acid (30% v/v) containing sodium cyanoborohydride (1 M). The glycan solution was then incubated at 65 °C for 2 h. After the conjugation with 2-AB, the reaction mixture was applied to a cellulose disc (1 cm in diameter) in a glass holder. The disc was washed five times with 1 mL of acetonitrile to remove non-oligosaccharide reactants. Labeled glycans were then eluted using two washes (0.5 mL) of water and then filtered (0.2 μm). The solution was dried and resuspended to 100 μL.

*Glycosidase Treatment of Oligosaccharides*. Separate aliquots (2 μL representing ∼7 pmol of β-subunit) of the PNGase F digest were treated for 18 h at 37 °C with combinations of the following glycosidases: (1) α-galactosidase from coffee beans (4 milliunits) in sodium acetate buffer (25 mM, pH 6.0) with a final volume of 4 μL; (2) α-galactosidase (4 milliunits) and chicken liver fucosidase

[1] Abbreviations: MALDI/MS, matrix-assisted laser desorption ionization mass spectrometry with time of flight detection; MALDI/CID; matrix-assisted laser desorption ionization with collision-induced dissociation; HPAEC/PAD, high-pH anion-exchange chromatography with pulsed amperometric detection; PNGase F, peptide-$N^4$-(*N*-acetyl-β-D-glucosaminyl)aspargine amidase; Endo H, *endo*-β-*N*-acetylglucosaminidase H; 2-AB, 2-aminobenzamide; DHB, 2,5-dihydroxybenzoic acid.

(2.8 milliunits) in sodium acetate buffer (20 mM, pH 6.0) with a final volume of 4 $\mu$L; (3) α-galactosidase (4 milliunits), chicken liver fucosidase (2.8 milliunits), and $\beta$-galactosidase (1.2 milliunits) in sodium acetate buffer (25 mM, pH 6.0) to a final volume of 4 $\mu$L.

*Endoglycosidase and Amidase Digestion of Glycopeptides*. Samples of each HPLC fraction were either analyzed directly by MALDI/MS or treated with PNGase F prior to MALDI/MS analysis. Two percent of each glycopeptide HPLC fraction was dried, resuspended in water, and incubated with either PNGase F (1 milliunits) in $NH_4HCO_3$ (25 mM, pH 8.0) or Endo H (1 milliunits) in sodium acetate (25 mM, pH 5.5) for 18 h in a total volume of 20 $\mu$l. The sample was directly used for MALDI/MS analysis. For sequential digests of glycopeptides with Endo H and PNGase F, 2% of the glycopeptide HPLC fraction was dried, resuspended in sodium acetate (25 mM, pH 5.5), and incubated with Endo H (1 milliunits) for 18 h in a total volume of 20 $\mu$L. The Endo H digest was then boiled for 5 min. To an aliquot (10 $\mu$L) of the Endo H digest was added $NH_4HCO_3$ (25 mM, pH 8.0) followed by PNGase F (1 milliunits), and the mixture was incubated overnight at 37 °C. All the samples were analyzed by MALDI/MS without further sample processing.

*Monosaccharide Analysis*. About 20% of each HPLC fraction was dried in a SpeedVac concentrator and analyzed for monosaccharides as previously described *(19*). Hydrolysis of neutral sugars was accomplished by the addition of 200 $\mu$L of 2 N TFA with incubation for 3 h at 100 °C. After hydrolysis, samples were immediately dried in a SpeedVac, dissolved in 200 $\mu$L of water, and then transferred to autosampler vials. All samples (150 $\mu$L) were analyzed for monosaccharides with the Dionex GlycoStationTM equipped with a CarboPac PA1 column (Dionex) (0.4 × 25 cm) and a CarboPac PA1 guard column (0.4 × 5 cm). The samples were separated isocratically with 16 mM NaOH over 25 min, followed by a 10 min elution with 200 mM NaOH and then a return to starting conditions for 15 min prior to the next injection. All separations used a flow rate of 1.0 mL/min. The hydrolyzates were quantified with an external monosaccharide standard mixture Fuc, GlcN, GalN, Gal, Glc, and Man. Data were collected and processed using the Dionex GlycoStationTM software.

*Peptide Sequence Analysis*. The amino terminal sequence was determined for fractions containing carbohydrate using an Applied Biosystems Gas-Phase sequencer system (model 740 A). Amounts of 20−30 pmol of each peptide were sequenced after deposition onto a glass fiber peptide support.

*MALDI/MS Analysis*. Matrix-assisted laser desorption ionization mass spectrometry (MALDI/MS) was carried out on a Micromass TofSpec SE using a nitrogen laser operated at 337 nm with a 3-ns pulse width. Measurements were performed in the positive-ion mode with an accelerating voltage of 22 or 25 kV except for one glycopeptide (GP4) where analysis was performed in the negative-ion mode (−22 kV). Spectra were the sum of 25−35 laser shots. A 2 $\mu$L aliquot of a peptide fraction, collected from HPLC, was mixed with 2 $\mu$L of α-cyano-4-hydroxycinnamic acid, vortexed, and centrifuged. A 1 $\mu$L amount of the mixture was spotted onto a target along with peptide standards. For analysis of oligosaccharides, 1 $\mu$l of oligosaccharide digest was mixed with 1 $\mu$L of 2,5-dihydroxybenzoic acid, vortexed and centrifuged. A 1 $\mu$L amount of the mixture was spotted onto a target. The higher masses (molecular weights > 2500 Da) were calibrated externally using a mixture containing bovine insulin oxidized B chain, human recombinant insulin, ubiquitin, and egg white lysozyme. For calibration in the lower mass region bombesin and the 18−39 clip of adrenocorticotropic hormone fragment (18−39) were used.

*Mass Composition Analysis*. The composition of oligosaccharides, in terms of Hex, HexNAc, and deoxyHex residues, was determined using a computer program written by Dr. Wade Hines, UCSF. All possible mass compositions were generated from the observed MALDI/MS masses (±8 Da). The monosaccharide compositions considered were those previously described (*11*).

*MALDI/MS with CID Analysis*. MALDI/CID experiments were carried out using a Micromass AutoSpec orthogonal acceleration time-of-flight (TOF) mass spectrometer equipped with a MALDI source (*20*). The $N_2$ laser (337 nm) wavelength was operated at 10 Hz pulse rate. MS-1 was tuned manually to transmit the $^{12}C$ monoisotopic ion of the precursor mass. The matrix was 2,5-dihydroxybenzoic acid.

## RESULTS

In previous studies it was determined that the *N*-linked oligosaccharides of the gastric $\beta$-subunit were oligomannosidic and neutral lactosamine-type, the latter terminated exclusively with GalαGal units (*12*). As an underpinning to understanding the glycobiology of the H,K-ATPase, studies were undertaken to localize the oligosaccharides to individual glycosylation sites. The structures of the total oligosaccharide pool were first determined using MALDI/MS and exoglycosidase analysis. Tryptic glycopeptides were then isolated and analyzed by MALDI/MS, and oligosaccharide structures were assigned to individual sites on the basis of mass increments to the peptide molecular weights.

*MALDI/MS with Exoglycosidase Analysis of Gastric $\beta$-Subunit Oligosaccharides*. Figure 1 shows the MALDI/MS spectrum of the total pool of 2-aminobenzamide (2-AB) labeled oligosaccharides from the gastric $\beta$-subunit (panel A), after digestion with either α-galactosidase (panel B), or α-galactosidase and α-fucosidase (panel C). Treatment with α-galactosidase (panel B) resulted in a shift of all signals greater than *m/z* 2000 by masses equal to the loss of two to six Hex residues, indicating that all the lactosamine-type oligosaccharides had α-Gal termini. Combined α-fucosidase and α-galactosidase digestion shifted the major signals by ∼146 Da (compare panels B and C), indicating that most of the lactosamine-type oligosaccharides contained a single Fuc residue. The signals at *m/z* 1174, 1336, 1498, and 1660 remained unaffected by the exoglycosidases and these signals corresponded, respectively, to the molecular weights of natriated adducts of 2-AB labeled $Man_5GlcNAc$, $Man_6GlcNAc$, $Man_7GlcNAc$, and $Man_8GlcNAc$ structures (Table 1, **Ia**−**Id**). The loss of the reducing end GlcNAc was attributed to the presence of trace amounts of Endo F contaminant in the PNGase F preparation.

To determine the antennarity of the oligosaccharides and the number of lactosamine extensions, the total pool of oligosaccharides was also treated simultaneously with α-galactosidase, α-fucosidase, and $\beta$-galactosidase (data not shown). The resulting "core structures" from considering all possible mass compositions with the known monosaccharides on the rabbit H,K-ATPase (Weitzahandler et al., 1992) are summarized in Chart 1. Signals observed at *m/z*

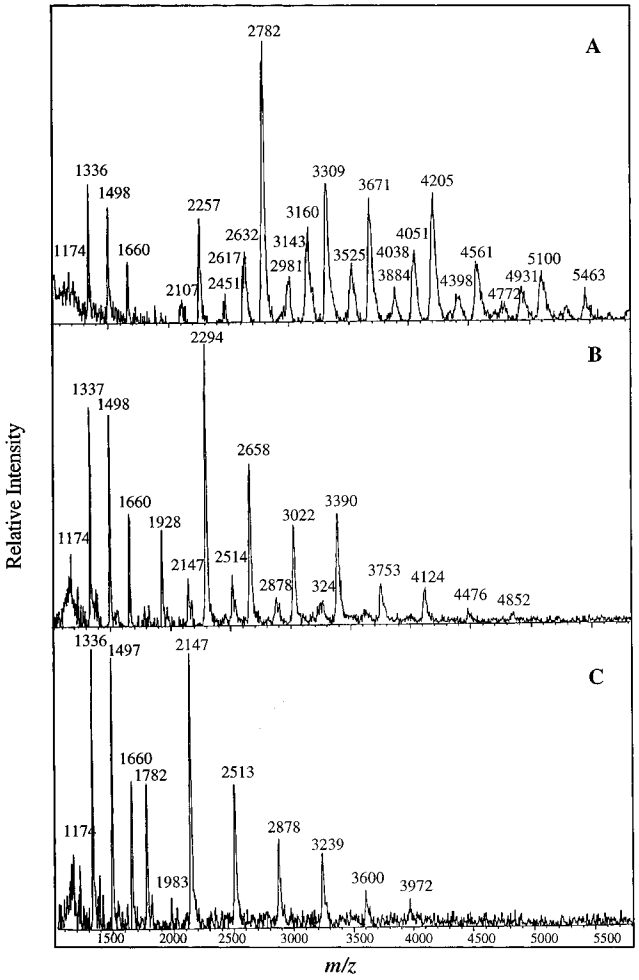


FIGURE 1: MALDI/MS analysis of exoglycosidase digestions of *N*-linked oligosaccharides from the rabbit $\beta$-subunit. The oligosaccharides, released by PNGase F digestion of the $\beta$-subunit, were derivatized with 2-aminobenzamide and digested with exoglycosidases as described under Materials and Methods. Aliquots of digests from ~3 pmol of protein, were then reanalyzed by MALDI/MS without further sample processing. (A) Untreated 2-AB-derivatized $\beta$-subunit oligosaccharides; (B) after digestion with α-galactosidase; (C) after treatment with α-galactosidase and α-fucosidase. All spectra were obtained in the positive ion mode using an accelerating voltage of 25 kV as detailed under Materials and Methods. The matrix used was 2,5-dihydroxybenzoic acid. Each spectrum represents oligosaccharides from ~1.5 pmol of the glycoprotein.

1458, 1824, and 2188 corresponded to agalacto-biantennary structures with none, one, or two lactosamine repeats, respectively. Signals at *m/z* 1660, 2027, 2394, and 2756 corresponded to agalacto-triantennary structures with none, one, two, or three lactosamine repeats, respectively. Signals at *m/z* 2592, 2960 and 3322 corresponded to tetrantennary structures with two, three, or four lactosamine repeats, respectively. The branch location of the lactosamine repeats cannot be determined from this analysis.

The individual structures of the native oligosaccharides were deduced from mass decrements after exoglycosidase digestions. For example, the signal at *m/z* 3143 (Figure 1A) corresponds to the mass of the core-fucosylated triantennary structure with one lactosamine repeat and three GalαGal termini (Table 1, **IIId**). After treatment with α-galactosidase, an expected signal from the loss of three Hex residues at *m/z* 2658 was observed (Figure 1B). After α-fucosidase digestion, the expected signal from the loss of a single Fuc residue at *m/z* 2513 was also observed (Figure 1, panel C).

Table 1: Structure of $\beta$-Subunit Oligosaccharides

| [M + Na$^+$] obsd[a] | [M + Na$^+$] calcd[b] | composition | structure[c] | no.[d] |
|---|---|---|---|---|
| 1174 | 1174 | $Hex_5HexNAc$ | | **Ia** |
| 1336 | 1336 | $Hex_6HexNAc$ | | **Ib** |
| 1498 | 1498 | $Hex_7HexNAc$ | | **Ic** |
| 1660 | 1661 | $Hex_8HexNAc$ | | **Id** |
| 2107, 2257 | 2108, 2254 | $Hex_7HexNAc_4±dHex_1$ | | **IIa, IIb** |
| 2451 | 2457 | $Hex_7HexNAc_5dHex_1$ | | **IIc** |
| 2471, 2617 | 2473, 2619 | $Hex_8HexNAc_5±dHex_1$ | | **IId, IIe** |
| 2981 | 2984 | $Hex_9HexNAc_6dHex_1$ | | **IIf** |
| 2632, 2782 | 2635, 2781 | $Hex_9HexNAc_5±dHex_1$ | | **IIg, IIh** |
| 2632, 2782 | 2635, 2781 | $Hex_9HexNAc_5±dHex_1$ | | **IIIa, IIIb** |
| 3005, 3143 | 3000, 3146 | $Hex_{10}HexNAc_6±dHex_1$ | | **IIIc, IIId** |
| 3160, 3309 | 3162, 3308 | $Hex_{11}HexNAc_6±dHex_1$ | | **IIIe, IIIf** |
| 3508 | 3511 | $Hex_{11}HexNAc_7dHex_1$ | | **IIIg** |
| 3525, 3671 | 3527, 3673 | $Hex_{12}HexNAc_7±dHex$ | | **IIIh, IIIi** |
| 3884 | 3876 | $Hex_{12}HexNAc_8dHex_1$ | | **IIIj** |
| 4038 | 4038 | $Hex_{13}HexNAc_8dHex_1$ | | **IVa** |
| 4051, 4205 | 4058, 4199 | $Hex_{14}HexNAc_8±dHex_1$ | | **IVb, IVc** |
| 4398 | 4403 | $Hex_{14}HexNAc_9dHex_1$ | | **IVd** |
| 4561 | 4565 | $Hex_{15}HexNAc_9dHex$ | | **IVe** |
| 4772 | 4768 | $Hex_{15}HexNAc_{10}dHex_1$ | | **IVf** |
| 4931 | 4930 | $Hex_{16}HexNAc_{10}dHex_1$ | | **IVg** |
| 5100 | 5092 | $Hex_{17}HexNAc_{10}dHex_1$ | | **IVh** |

[a] The masses correspond to the signals observed in Figure 1A. [b] The massess include the mass of the 2-AB label. [c] □, GlcNAc; ○, Man; open triangles, $\beta$-Gal; ovals, Fuc; and solid triangles, α-Gal residues. The high-mannose oligosaccharides are depicted with two GlcNAc's, and the loss of a GlcNAc at the reducing end, as indicated by the mass/composition analysis, was attributed to Endo F activity in the PNGase F preparation. The branch location of the lactosamine repeats and the location of the additional α-Gal residues are not known. [d] In cases where two masses are indicated, the second number represents the fucosylated species.

On subsequent treatment with $\beta$-galactosidase an expected signal at *m/z* 2027 for an agalacto-triantennary core oligosaccharide (Chart 1) was also observed (data not shown). Using a similar strategy, structures with a single Gal$\alpha$Gal$\beta$ unit per branch were assigned (Table 1, **IIb**,**c**,**e**,**f**, **IIIb**,**d**,**g**,**j**, and **IVa**,**d**,**f**).

The mass composition analysis of signals at *m/z* 3160, 3309, 3525, 3671, 4051, 4205, 4561, 4931, and 5100 suggested structures with additional terminal Hex residues.

Chart 1: $\beta$-Subunit Oligosaccharides after Simultaneous Treatment with α-Galactosidase, $\beta$-Galactosidase, and α-Fucosidase[a]

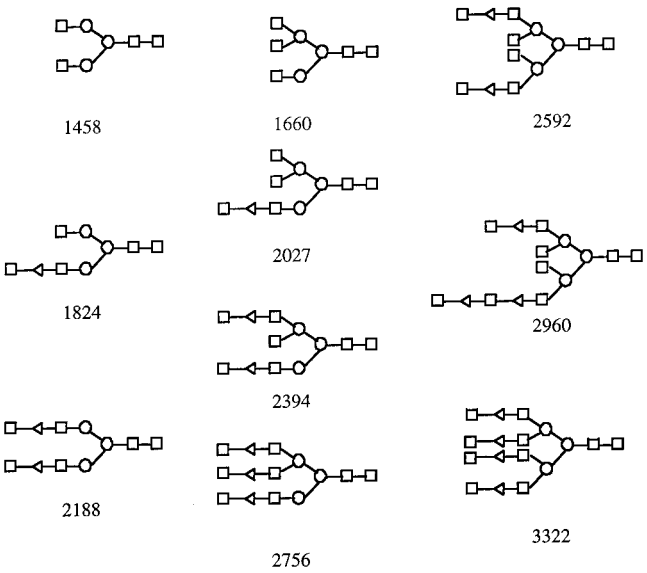


[a] □, GlcNAc; ○, Man; ▽, Gal. The branch location of the lactosamine repeats is not known.

The digestion data verified that these "excess" Hex residues were in α-Gal linkages, which would theoretically correspond to novel structures with multiple α-Gal residues per branch. These structures were assigned from mass composition analysis and masses after exoglycosidase digestions. For example, the signal at *m/z* 3309 corresponds to the mass of either a tetraantennary oligosaccharide or to a triantennary oligosaccharide with a lactosamine repeat and an additional Hex residue (**IIIf**), both core fucosylated and with GalαGal termini. Both signals would lose four Hex residues after treatment with α-galactosidase and give a signal at *m/z* 2658, as observed (Figure 1B). However, triantennary and tetraantennary structures would lose three and four Hex residues after $\beta$-galactosidase treatment, producing signals at *m/z* 2027 and 1866, respectively (after defucosylation). Since only the signal at *m/z* 2027 was observed (data not shown), we concluded that the parent signal represented only a core-fucosylated triantennary oligosaccharide with one lactosamine repeat and four α-Gal termini (Table 1, **IIIf**), a novel structure. Using similar logic, other structures with multiple α-Gal residues per branch were assigned (**IIg**,**h**, **IIIe**,**f**,**h**,**i**, and **IVb**,**c**,**e**,**g**,**h**). The branch location of the additional α-Gal residues cannot be deduced from these data.

All the major signals shifted by ∼146 Da on treatment with α-fucosidase; however, minor signals at *m/z* 2147, 2514, and 2878, which corresponded to non-fucosylated structures were observed prior to α-fucosidase treatment (Figure 1, B and C). It was also observed that native oligosaccharides gave broader signals, and when examined in detail were found to represent multiple signals. For example, the signal at *m/z* 2632 is a non-fucosylated triantennary oligosaccharide with α-Gal termini (**IIIa**) while the neighboring signal at *m/z* 2617 is a fucosylated biantennary oligosaccharide with a single lactosamine repeat and α-Gal termini (**IIe**). Similarly, other non-fucosylated structures were assigned (**IIa**,**d**,**g**, **IIIa**,**c**,**e**,**h**, and **IVb**).

As described above, the digestion data enabled assignments of unique structures from the possibilities produced by mass composition analysis. However, in two cases the structures could not be resolved. The signal at *m/z* 2632 corresponds to a non-fucosylated triantennary oligosaccharides with α-Gal termini (**IIIa**) or to a biantennary oligosaccharide with a single lactosamine repeat and three α-Gal termini (**IIg**). Both structures would lose three Hex residues after α-galactosidase treatment, and a corresponding signal at *m/z* 2146 was observed. A biantennary and triantennary structure would lose two and three Hex residues after $\beta$-galactosidase treatment, producing signals at *m/z* 1823 and 1662, respectively (after defucosylation). While, a signal at *m/z* 1824 was observed, the signal at *m/z* 1662 was obscured by the ion from $Man_8GlcNAc$ (*m/z* 1658), hence neither structural possibility could be eliminated. Hence, the signal at *m/z* 2632 was assigned to both structures (**IIg** and **IIIa**). Similarly, the signal at 2782 corresponds to a fucosylated triantennary oligosaccharides with α-Gal termini (**IIIa**) or to a fucosylated biantennary oligosaccharide with a single lactosamine repeat and three α-Gal termini (**IIh**). Both structures would lose three Hex residues after α-galactosidase treatment, and corresponding signals at *m/z* 2296 were observed. A biantennary and triantennary structure would lose two and three Hex residues after $\beta$-galactosidase treatment, producing signals at *m/z* 1823 and 1662, respectively (after defucosylation). While a signal at *m/z* 1824 was observed, the signal at *m/z* 1662 was obscured by the signal for $Man_8GlcNAc$ (*m/z* 1658), hence neither structural possibility could be eliminated. Hence the signal at *m/z* 2632 was assigned to both structures (**IIh** and **IIIb**).

From the combination of MALDI/MS, mass composition analysis, and exoglycosidase digestions, bi-, tri-, and tetraantennary structures with all branches terminated in α-Gal residues were identified in the total oligosaccharide pool from the gastric $\beta$-subunit. Of these, 17 were core-fucosylated lactosamine-type oligosaccharides and seven were non-fucosylated structures. From the shifts in mass on treatment with α-galactosidase, the oligosaccharide pool included nine structures with multiple α-Gal residues on a single oligosaccharide branch. The presence of four oligomannosidic structures was also verified (*12*).

*Oligosaccharide Localization on the Gastric $\beta$-Subunit.* The distribution of oligosaccharide structures (Table 1) among the *N*-linked sequons was determined next. The purified gastric $\beta$-subunit from rabbit H,K-ATPase (∼1 nmol) was digested with trypsin, and the peptides were separated by reversed phase HPLC (Figure 2A). Forty individual fractions were collected, and an aliquot equivalent to ∼200 pmol of protein was analyzed for monosaccharide content by HPAEC-PAD. The amounts of Gal and GlcNAc in each fraction is shown in Figure 2B. Fractions 4, 7, 8, 10, 16, 18, 19, 27, 33, and 35 showed greater amounts of Gal and GlcNAc than the other fractions (Figure 2B). The carbohydrate-containing fractions were treated as glycopeptides and analyzed further. An aliquot of each fraction (∼4 pmol) was analyzed by MALDI/MS using α-cyano-4-hydroxycinnamic acid as a matrix. Peptides covering 85% of the $\beta$-subunit sequence were also identified by molecular weight using MALDI/MS (data not shown). The GP1−GP7 fractions from HPLC showed signals at *m/z* 4000−6000 Da which differed by masses characteristic of sugar residues (e.g., Hex, 162 Da; HexNAc, 203 Da; or deoxyHex, 146 Da) or a combination of these masses. Each of these glycopeptide fractions was analyzed by MALDI/MS before

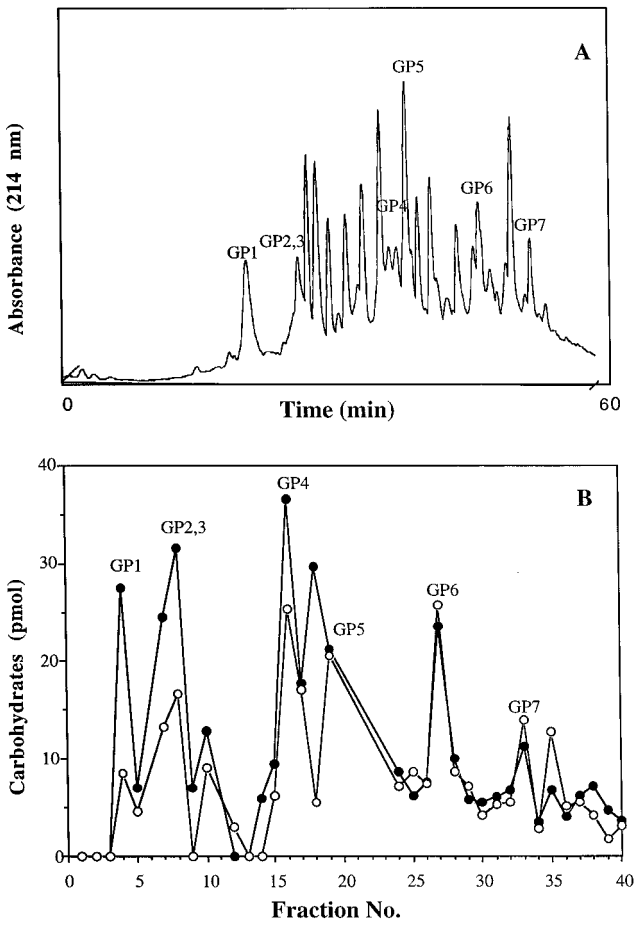


FIGURE 2: Reversed phase HPLC of the rabbit β-subunit tryptic digest (A) and monosaccharide analysis of peak fractions (B). The tryptic digest of the reduced and alkylated β-subunit was analyzed by RP/HPLC (A), as described under Materials and Methods. Approximately 200 pmol of each fraction was subjected to hydrolysis with 2 N TFA and analyzed by HPAEC/PAD (B). The quantitation of GlcNAc (○) and Gal (●) in each HPLC fraction is shown. The peaks demonstrating >10 pmol of Gal were indicated as GP1−GP7.

and after treatment with either PNGase F or Endo H, as described below.

*Oligosaccharides at Asn[193]*. The MALDI/MS spectrum of GP1 (Figure 3A) showed the presence of a series of masses *m/z* 2169, 2333, 2496, 2658, and 2820 which differed by ∼162 Da, suggesting that GP1 contained a peptide modified by the oligomannose structures. Digestion with Endo H resulted in the apparent disappearance of all signals greater than *m/z* 2000 and the appearance of a signal at *m/z* 1318 and its natriated product *m/z* 1340 (Figure 3B). The results show that GP1 is modified with oligomannose sugars. Deglycosylation of GP1 with PNGase F followed by analysis with MALDI/MS gave rise to a peptide at *m/z* 1117, which corresponded to the mass of deglycosylated tryptic peptide, Phe[189]−Arg[198], 1117.2 Da (Figure 3C). The calculated mass for all PNGase F deglycosylated peptides accounted for the enzymatic conversion of Asn to Asp at glycosylated sites. The signal at *m/z* 1318 is the mass of the core peptide (1116.2 Da) and one HexNAc residue. Edman degradation of GP1 verified the sequence as Phe[189]−Arg[198] of the gastric β-subunit (Table 2). A blank was at the Asn residue, confirming that Asn[193] is glycosylated. From the mass increments to the peptide molecular weight, the signals at *m/z* of 2169, 2333, 2496, 2658, and 2820 were respectively assigned to glycopeptides containing $Man_4GlcNAc_2$, $Man_5GlcNAc_2$ (**Ia**, Table 1), $Man_6GlcNAc2$ (**Ib**), $Man_7GlcNAc_2$ (**Ic**), and $Man_8GlcNAc_2$ (**Id**) species linked to Phe[189]−Arg[198] (Table 3). No signal corresponding to $Man_9GlcNAc_2$ was seen.

Lower intensity signals at higher *m/z* values, which differed by combinations of 162 and 203 Da (*m/z* 3210, 3572, and 3737 Da), were also observed (Figure 3A). These signals remained after Endo H treatment (Figure 3B, see inset), indicating that they were not oligomannosidic/hybrid oligosaccharides. Since the only signal that appeared on PNGase F treatment was at *m/z* 1117 Da, it was concluded that the fraction did not contain glycopeptides from other sites. Subtraction of 1117 Da from the higher masses gave masses consistent with $Hex_7HexNAc_4deoxyHex$, $Hex_8HexNAc_5deoxyHex$, and $Hex_9HexNAc_5deoxyHex$, respectively, which corresponded to a core-fucosylated biantennary structure with α-Gal termini (**IIb**), the same structure with an additional lactosamine unit (**IIe**), and a core-fucosylated triantennary oligosaccharide with all branches terminated in GalαGal residues (**IIIb**). Thus, Asn[193] is modified with both oligomannose and lactosamine-type oligosaccharide chains.

*Oligosaccharides at Asn[99] and Asn[103]*. The MALDI/MS analysis of GP2,3 is shown in Figure 4, trace A. A series of signals at *m/z* 4734, 4900, 5060, 5222, 5430, 5591, and 5753 were observed. PNGase F treatment of GP2,3 resulted in the appearance of a single major signal at *m/z* 1432 (Figure 4, trace D) which is the mass of the deglycosylated tryptic peptide Gly[93]−Arg[104]. Edman sequencing confirmed that the peptide was Gly[93]−Arg[104] of the gastric β-subunit (Table 2). Two potential *N*-linked glycoylation sites Asn[99] and Asn[103] are in this sequence. Edman sequencing showed blanks at both positions 99 and 103, indicating that both Asn residues are glycosylated.

Endo H digestion was next performed on GP2,3 to determine if any of the sites were glycosylated with oligomannosidic/hybrid structures. Figure 4, trace B, shows the disappearance of the entire higher mass complex (*m/z* 4700−6000) and the appearance of major new signals at *m/z* 3731, 4102, and 4261, which differed in mass by combinations of Hex and HexNAc residues. A signal corresponding to the mass of the peptide plus two GlcNAc residues (*m/z* 1837) was not observed. These results suggest that only one of the sites is glycosylated with oligomannose structures, and the signals, observed after Endo H treatment, are from the contributions of lactosamine-type chains at the second site. To ascertain if GP2,3 is modified by oligomannosidic glycans at both sites, the glycopeptide was first treated with Endo H and then with PNGase F. Figure 4, trace C, shows the appearance of a single peak at *m/z* 1634 which corresponds to the mass of the peptide Gly[93]−Arg[104] (1432 Da) modified with a single GlcNAc residue, thus indicating that a single glycoform of these glycopeptides has only one site modified by oligomannosidic/hybrid structures.

To determine whether Asn[99] or Asn[103] or both bear oligomannosidic structures, GP2,3 was treated with V8 protease. The Asp residue between the two glycosylated sites was resistant to hydrolysis. MALDI/CID analysis was therefore utilized to identify which sequon(s) was modified by oligomannosidic structures. The GP2,3 glycopeptide was first treated sequentially with Endo H and then with PNGase F. This treatment produced glycopeptides in which one Asn residue with oligomannosidic structures was modified by a

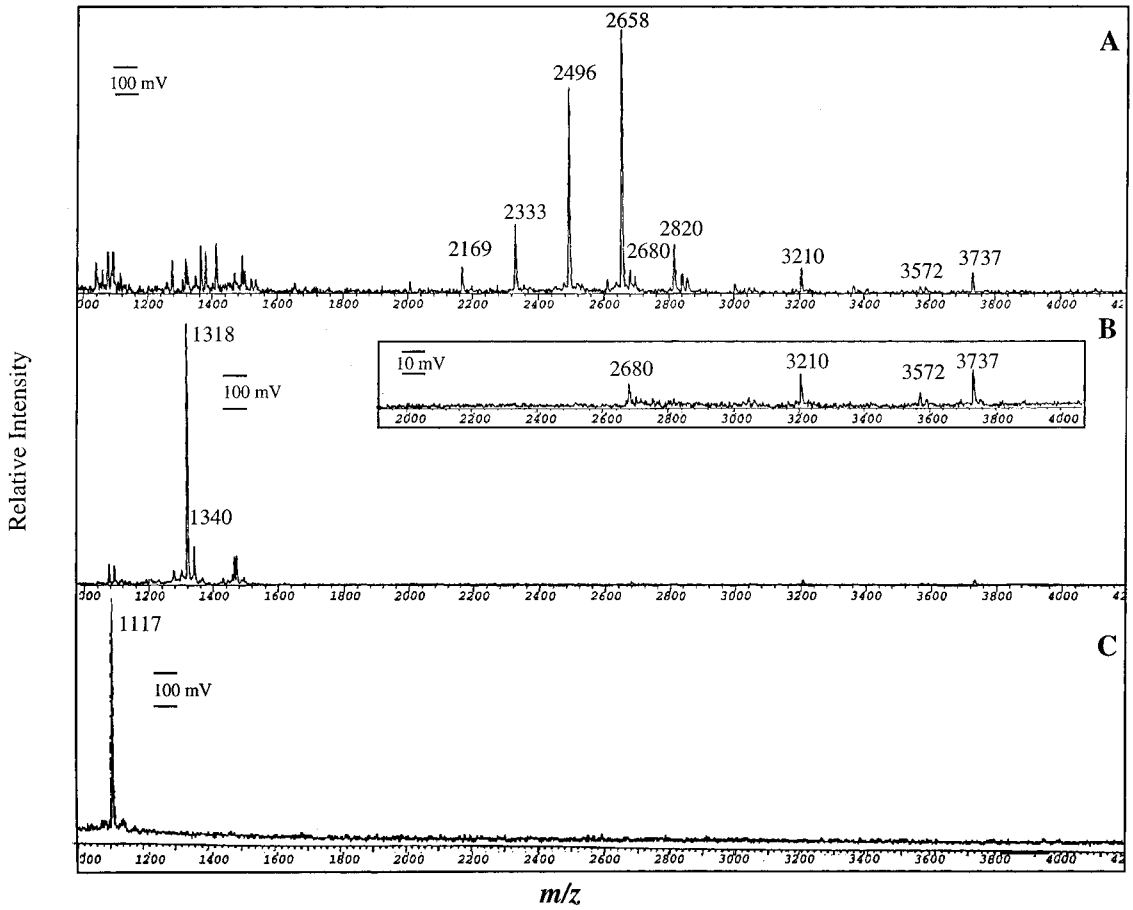


FIGURE 3: MALDI/MS analysis of glycopeptide GP1. GP1 was prepared by RP/HPLC of the gastric $\beta$-subunit tryptic digest. GP1 (20 pmol) was treated with PNGase F or Endo H as described in Materials and Methods, and ~2 pmol of the digest was analyzed by MALDI/MS utilizing α-cyano-4-hydroxycinnamic acid as a matrix. (A) GP1 before treatment; (B) GP1 after treatment with Endo H; and (C) GP1 after treatment with PNGase F. The inset details the spectrum in the range *m/z* 2000−4000 after Endo H treatment. All the spectra were from the sum of 25−30 laser shots in the positive ionization mode.

Table 2: Edman Sequence Analysis of Gastric $\beta$-Subunit Glycopeptides

| glycopeptide | glycosylation site | experimental sequence | tryptic peptides[a] |
|---|---|---|---|
| GP1 | Asn[193] | FLPSXSTPPR | [189]FLPSNSTPPR[198] |
| GP2,3 | Asn[99,103] | (G,A)LEIHYXISDXR | [93]GLEIHYNISDNR[104] |
| GP4 | Asn[130] | SFLAGYSPAAQVDNIXBXX | [115]SFLAGYSPAAQVDNINBTSK[134] |
| GP5 | Asn[146] | TYFFQESFGAPXHTK | [135]TYFFQESFGAPNHTK[149] |
| GP6 | Asn[161] | FTADMLEXBSGLTDP... | [154]FTADMLENBSGLTDPSFGFK[174] |
| GP7 | Asn[222] | XDBTFLDMPHQAL(D)PLQVEYYP... | [199]VDBTFLDMPHQALTPLQVEYYPPNGTFSLHFPYYGK[235] |

[a] B refers to carboxymethylated cysteines.

GlcNAc and the other Asn was converted to an Asp residue, observed at *m/z* 1634 (Figure 4, trace C). The monoisotopic signal at *m/z* 1634.9 was selected for CID analysis as shown in Figure 5. The carboxy-terminal ion, $\mathbf{y_2}$, which is formed by a peptide bond cleavage between Asp[102] and the newly formed Asp[103] was detected at *m/z* 290. The unmodified $\mathbf{y_3}$, $\mathbf{v_4}$, $\mathbf{w_5}$, and $\mathbf{Y_5}$ ions at *m/z* 405, 460, 570, and 603 confirmed that Asn[103] does not bear oligomannosidic structures. No ions corresponding to a GlcNAc modification at Asn[103] were seen. However, a $\mathbf{y_6}$ ion (peptide bond cleavage between His[98] and Asn[99]) with a 203 Da mass increment was seen at *m/z* of 922. Similarly, $\mathbf{y_7}$-$H_2O$, $\mathbf{v_7}$, $\mathbf{v_8}$, and $\mathbf{v_9}$ were seen at *m/z* 1068, 978, 1141, and 1278, respectively, all of which had a 203 Da greater mass from the modification of Asn[99] with a GlcNAc. These results unambiguously show that Asn[99] is modified with oligomannosidic glycans and Asn[103] is modified by lactosamine-type oligosaccharides. With these results the oligosaccharides on Asn[99] and Asn[103] were assigned. The Asn[99] residue is modified with $Man_5GlcNAc_2$ (**Ia**), $Man_6GlcNAc_2$ (**Ib**), $Man_7GlcNAc_2$ (**Ic**), and $Man_8GlcNAc_2$ (**Id**) (Table 3) oligosaccharides. The mass compositions of the lactosamine-type structures at Asn[103] correspond to a biantennary structure (**IIb**), a biantennary with a lactosamine repeat (**IId**) and a triantennary (**IIIb**) oligosaccharide, all three core fucosylated and with all branches terminated in GalαGal residues (Table 1).

*Oligosaccharides at Asn[130]*. Figure 6A shows the MALDI/MS of GP4 in the negative ionization mode. Signals at *m/z* 4767, 4924, 5131, 5296, 5458, 5656, 6017, 6181, 6552, and 6706 were observed. The core peptide obtained on PNGase F treatment was observed at a *m/z* 2145 (data not shown), which is the predicted mass of the deglycosylated peptide Ser[115]−Lys[134] (2146 Da) of the gastric $\beta$-subunit. Edman sequencing (Table 2) confirmed the identity of the peptide, and Asn[130] gave a blank in the sequencing cycle. The oligosaccharide masses at GP4 were determined by subtract-

Table 3: Oligosaccharide Structures at *N*-Linked Glycosylation Sites of the Gastric $\beta$-Subunit

| glycopeptide masses | | | | glycopeptide masses | | | |
|---|---|---|---|---|---|---|---|
| observed | calculated | mass composition[a] | oligosaccharide structures[b] | observed | calculated | mass composition[a] | oligosaccharide structures[b] |
| (GP1), $Asn^{193}$, $[M + H]^+$ | | | | (GP5), $Asn^{146}$, $[M + H]^+$ | | | |
| 2169 | 2171 | $Hex_4HexNAc_2$ | **$Man_4GlcNAc_2$** | 3703 | 3707 | $Hex_6HexNAc_4dHex$ | **IIb-Hex** |
| 2333 | 2334 | $Hex_5HexNAc_2$ | **Ia** | 3873 | 3869 | $Hex_7HexNAc_4dHex$ | **IIb** |
| 2496 | 2496 | $Hex_6HexNAc_2$ | **Ib** | 4077 | 4072 | $Hex_7HexNAc_5dHex$ | **IIc** |
| 2658 | 2658 | $Hex_7HexNAc_2$ | **Ic** | 4242 | 4234 | $Hex_8HexNAc_5dHex$ | **IIe** |
| 2680 | 2683 | $Hex_5HexNAc_3dHex$ | **IIb-$Hex_2$HexNAc** | 4397 | 4396 | $Hex_9HexNAc_5dHex$ | **IIIb/IIh** |
| 2820 | 2820 | $Hex_8HexNAc_2$ | **Id** | 4595 | 4600 | $Hex_9HexNAc_6dHex$ | **IIf** |
| 3210 | 3210 | $Hex_7HexNAc_4dHex$ | **IIb** | 4764 | 4762 | $Hex_{10}HexNAc_6dHex$ | **IIId** |
| 3572 | 3577 | $Hex_8HexNAc_5dHex$ | **IIe** | 4923 | 4924 | $Hex_{11}HexNAc_6dHex$ | **IIIf** |
| 3737 | 3738 | $Hex_9HexNAc_5dHex$ | **IIIb** | | | | |
| (GP2,3), $Asn^{99,103}$, $[M + H]^+$ | | | | (GP6), $Asn^{161}$, $[M - H]^-$ | | | |
| 4734 | 4743 | $Hex_{12}HexNAc_6dHex$ | **Ia**+**IIb** | 4168 | 4169 | $Hex_6HexNAc_4dHex$ | **IIb-Hex** |
| 4900 | 4905 | $Hex_{13}HexNAc_6dHex$ | **Ib**+**IIb** | 4330 | 4332 | $Hex_7HexNAc_4dHex$ | **IIb** |
| 5060 | 5067 | $Hex_{14}HexNAc_6dHex$ | **Ic**+**IIb** | 4533 | 4535 | $Hex_7HexNAc_5dHex$ | **IIc** |
| 5222 | 5229 | $Hex_{15}HexNAc_6dHex$ | **Id**+**IIb** | 4690 | 4697 | $Hex_8HexNAc_5dHex$ | **IIe** |
| 5430 | 5433 | $Hex_{15}HexNAc_7dHex$ | **Ib**+**IIIb** | 4892 | 4900 | $Hex_8HexNAc_6dHex$ | **IIe**+**HexNAc** |
| 5591 | 5596 | $Hex_{16}HexNAc_7dHex$ | **Ic**+**IIIb** | 4856 | 4859 | $Hex_9HexNAc_5dHex$ | **IIIb/IIh** |
| 5753 | 5758 | $Hex_{17}HexNAc_7dHex$ | **Id**+**IIIb** | 5057 | 5062 | $Hex_9HexNAc_6dHex$ | **IIf** |
| | | | | 5215 | 5224 | $Hex_{10}HexNAc_6dHex$ | **IIId** |
| (GP4), $Asn^{130}$, $[M - H]^-$ | | | | 5384 | 5386 | $Hex_{11}HexNAc_6dHex$ | **IIIf** |
| 4767 | 4765 | $Hex_9HexNAc_5dHex$ | **IIIb** | 5587 | 5590 | $Hex_{11}HexNAc_7dHex$ | **IIIg** |
| 4924 | 4927 | $Hex_{10}HexNAc_5dHex$ | **IIIb**+**Hex** | | | | |
| 5131 | 5130 | $Hex_{10}HexNAc_6dHex$ | **IIId** | | | | |
| 5296 | 5292 | $Hex_{11}HexNAc_6dHex$ | **IIIf** | | | | |
| 5458 | 5456 | $Hex_{12}HexNAc_6dHex$ | **IIIf**+**Hex** | | | | |
| 5656 | 5658 | $Hex_{12}HexNAc_7dHex$ | **IIIi** | | | | |
| 6017 | 6023 | $Hex_{13}HexNAc_8dHex$ | **IVa** | | | | |
| 6181 | 6185 | $Hex_{14}HexNAc_8dHex$ | **IVc** | | | | |
| 6552 | 6551 | $Hex_{15}HexNAc_9dHex$ | **IVe** | | | | |
| 6706 | 6713 | $Hex_{16}HexNAc_9dHex$ | **IVe**+**Hex** | | | | |

[a] Determined after subtraction of the molecular weight of the core peptide for the respective glycopeptide as described in the text. [b] The numbers refer to the oligosaccharide structures shown in Table 1.

ing the peptide molecular weight from the glycopeptide masses (Table 3). The oligosaccharide masses were assigned to structures deduced by exoglycosidase and MALDI/MS analysis. It was found that $Asn^{130}$ is glycosylated with (i) core-fucosylated triantennary structures (Table 1, **IIIb**); (ii) tri- and tetraantennary glycans with lactosamine units (**IIId**, **IIIf**, **IIIf**+**Hex**, **IIIi**, **IVa**, **IVc**, **IVe**, and **IVe**+**Hex**); (iii) structures with additional Hex residues per branch (**IIIb**+**Hex**, **IIIf**+**Hex**, **IIIi**, **IVc**, **IVe**, and **IVe**+**Hex**) where additional Hex masses are α-Gal-linked residues (Figure 1). Three structures with additional Hex residues (Table 3, **IIIb** +**Hex**, **IIIf**+**Hex**, and **IVe**+**Hex**) were not observed in the total oligosaccharide pool.

*Oligosaccharides at $Asn^{146}$ and $Asn^{161}$*. Figure 6B shows the MALDI/MS spectrum of GP5 in the positive ionization mode, and the major signals were observed at *m/z* 3873, 4077, 4242, 4397, 4595, 4764, and 4923. Deglycosylation with PNGase F resulted in a core peptide of *m/z* 1776 which corresponded to the mass of the deglycosylated peptide, $Thr^{135}$−$Lys^{149}$, which contains $Asn^{146}$ (data not shown). Edman analysis verified the sequence of the peptide (Table 2). From the oligosaccharide masses (Table 3) it was concluded that $Asn^{146}$ is primarily glycosylated with core-fucosylated biantennary (Table 1, **IIb**), biantennary with lactosamine repeats, (**IIe** and **IIf**), triantennary (**IIIb**), and triantennary with lactosamine repeats (**IIId** and **IIIf**). All the branches terminated with α-Gal extensions. A triantennary core-fucosylated structure with four α-Gal residues (**IIIf**) was also seen at this site.

Figure 6C shows the MALDI/MS spectrum of GP6 in the negative ionization mode. Signals at *m/z* 4168, 4330, 4533, 4690, 4856, 4892, 5057, 5215, 5384, and 5587 were observed. Edman sequencing revealed this peptide to be $Thr^{154}$−$Lys^{172}$ (Table 2). Deglycosylation with PNGase F resulted in the appearance of a peptide of mass 2254 Da which is 15 Da higher than the predicted mass of 2239. The difference is likely due to oxidation of the methionine residue in the peptide. Assignment of the oligosaccharide mass compositions (Table 3) revealed that $Thr^{154}$−$Lys^{172}$ is primarily glycosylated with fucosylated biantennary (Table 1, **IIb**), biantennary with lactosamine repeats (**IIe** and **IIf**), triantennary (**IIIb**), and triantennary with lactosamine repeats (**IIId**, **IIIf**, and **IIIg**) oligosaccharides, all the above being α-Gal-terminated structures. A triantennary core-fucosylated structure with multiple α-Gal residues was also seen at this site (**IIIf**).

*Characterization of GP7*. Fraction GP7 was identified as a glycopeptide by monosaccharide analysis (Figure 2B). When the MALDI/MS spectrum of GP 7 fraction was recorded, no peaks characteristic of glycopeptides were observed. In order to verify that the GP 7 fraction contained a glycopeptide, an aliquot was subjected to PNGase F digestion and then MALDI/MS was performed. The MALDI/MS analysis showed two new peaks at *m/z* 4987 and 4826 which were absent in the undigested sample (data not shown). GP7 was subjected to Edman sequencing, and the first 22 cycles gave the sequence contained in the $Val^{199}$−$Asn^{235}$ tryptic peptide (which contains $Asn^{222}$) of the $\beta$-subunit (Table 2). The calculated molecular weight of the PNGase F treated tryptic peptide $Val^{199}$−$Lys^{235}$ is 4412 Da. The mass obtained on PNGase F digestion corresponded to the addition of a $HexNAc_2$ and $HexNAc_2Hex$ to the $Val^{199}$−$Lys^{235}$

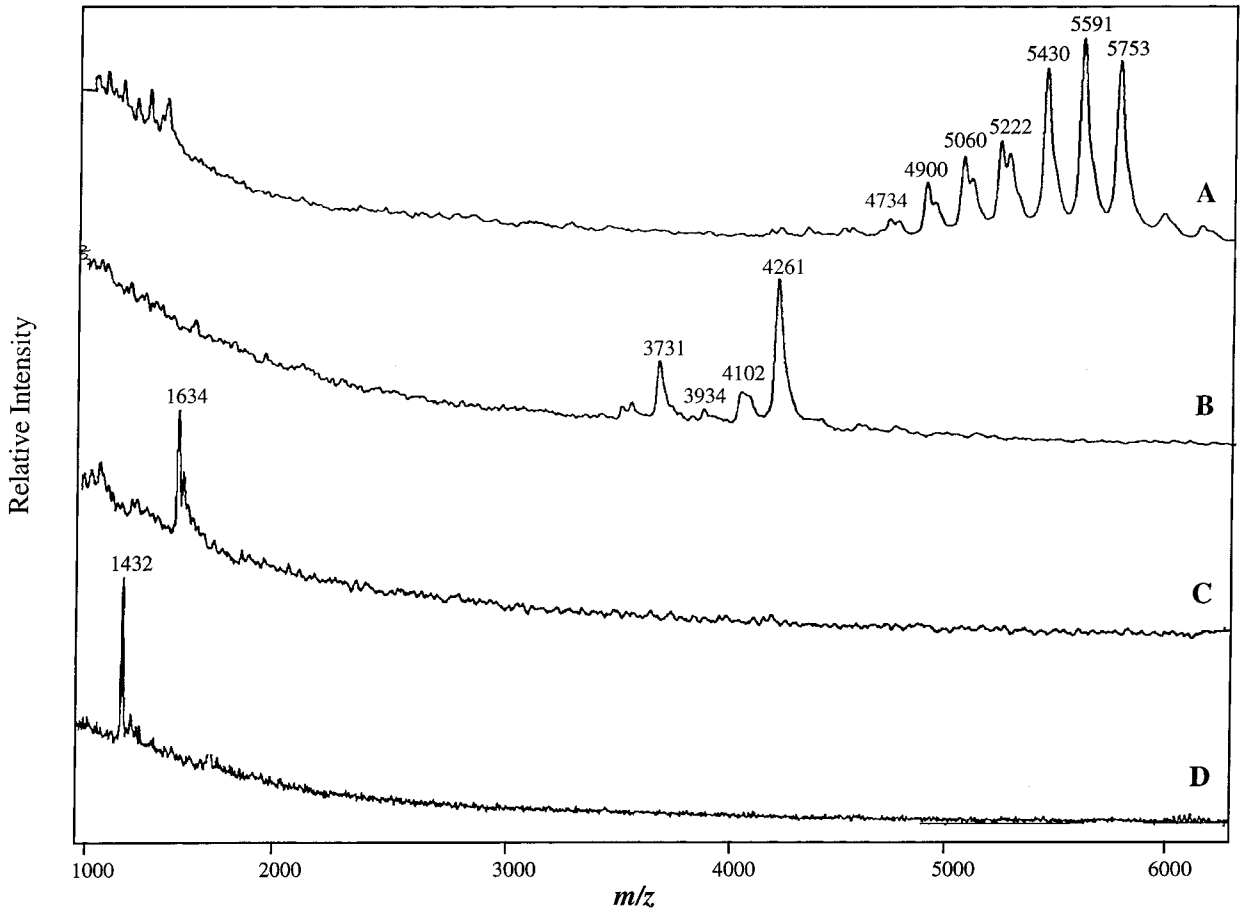


FIGURE 4: MALDI/MS analysis of glycopeptide GP2,3 after treatment with Endo H and PNGase F. GP2,3 (20 pmol) was treated with PNGase F and Endo H as described in Materials and Methods. Trace A, GP2,3 before treatment; trace B, after treatment with Endo H; trace C, after treatment with Endo H and then by PNGase F; and Trace D, after PNGase F digestion. The spectra were from 25 laser shots in the positive ionization mode. The glycopeptide (~4 pmol) was mixed with α-cyano-4-hydroxycinnamic acid as a matrix, and ~2 pmol was applied to the target.

peptide. Previous studies have shown the presence of GalNAc on the $\beta$-subunit (Weitzhandler et al., 1992), and the above results suggest that $Val^{199}$−$Lys^{235}$ is *O*-glycosylated. Further, $Thr^{212}$ was not seen in the sequencing cycle, suggesting that $Thr^{212}$ is *O*-glycosylated. Different matrices and conditions were tried in order to obtain a mass spectrum of GP7 glycopeptides, but no spectrum characteristic of glycopeptides was observed using either MALDI/MS or LC-ESI/MS.

## DISCUSSION

An understanding of the role of covalently linked carbohydrate in the function of the gastric H,K-ATPase requires localization of the oligosaccharides on the $\beta$-subunit. We have used a combination of monosaccharide analysis, exoglycosidase digestions, Edman sequencing, MALDI/MS, and tandem MS to determine the array of oligosaccharides at AsnX(Ser/Thr) sequons in the $\beta$-subunit of the gastric H,K-ATPase (Figure 7). All of the Asn residues in the seven sequons for *N*-glycosylation (residues 99, 103, 130, 146, 161, 193, and 222) were fully modified. To determine the structures in the total pool of oligosaccharides, unfractionated, PNGase F-released, oligosaccharides were first analyzed using MALDI/MS and exoglycosidase digestions. Both oligomannosidic ($Man_{5-8}GlcNAc_2$) and lactosamine-type bi-, tri-, and tetraantennary structure oligosaccharides were found. The major lactosamine-type structures contained one Fuc residue; however, minor MALDI/MS signals corresponding to non-fucosylated structures were also observed. Some of the bi-, tri-, and tetraantennary oligosaccharides contained 1−4 lactosamine repeats, and the branches of all of these structures were terminated in α-linked Gal residues. The data also indicated novel structures which had multiple α-linked Gal termini in a single branch. An unusually restricted site-specific distribution of structures was observed (Figure 7), with oligomannosidic structures at $Asn^{99}$ and a neighboring sequon $Asn^{103}$ containing lactosamine-type structures. $Asn^{193}$ contained both oligomannosidic and lactosamine-type oligosaccharides. Only lactosamine-type structures were found at $Asn^{130}$, $Asn^{146}$, and $Asn^{161}$. Most of the novel polylactosamine structures with more than one α-Gal residue per branch were observed at $Asn^{130}$.

Although the site distribution of oligosaccharides has been determined for a minority of glycoproteins, these studies have provided clues to the effect of protein structure on the activity of biosynthetic glycosidases and glycosyltransferases (*21*−*23*). The restricted arrays of oligosaccharides at each *N*-glycosylation site on the H,K-ATPase suggests precise site-dependent constraints on oligosaccharide biosynthesis of a membrane glycoprotein in its native cell type. All seven sequons were found to be fully glycosylated, and thus the initial transfer of the $Glc_3Man_9GlcNAc_2$ to all sequons was complete. Two sites ($Asn^{99}$ and $Asn^{193}$) contained oligomannosidic structures, suggesting inaccessibility to mannosidases which produce the oligosaccharide substrate that initiates lactosamine-type biosynthesis. Previous studies have

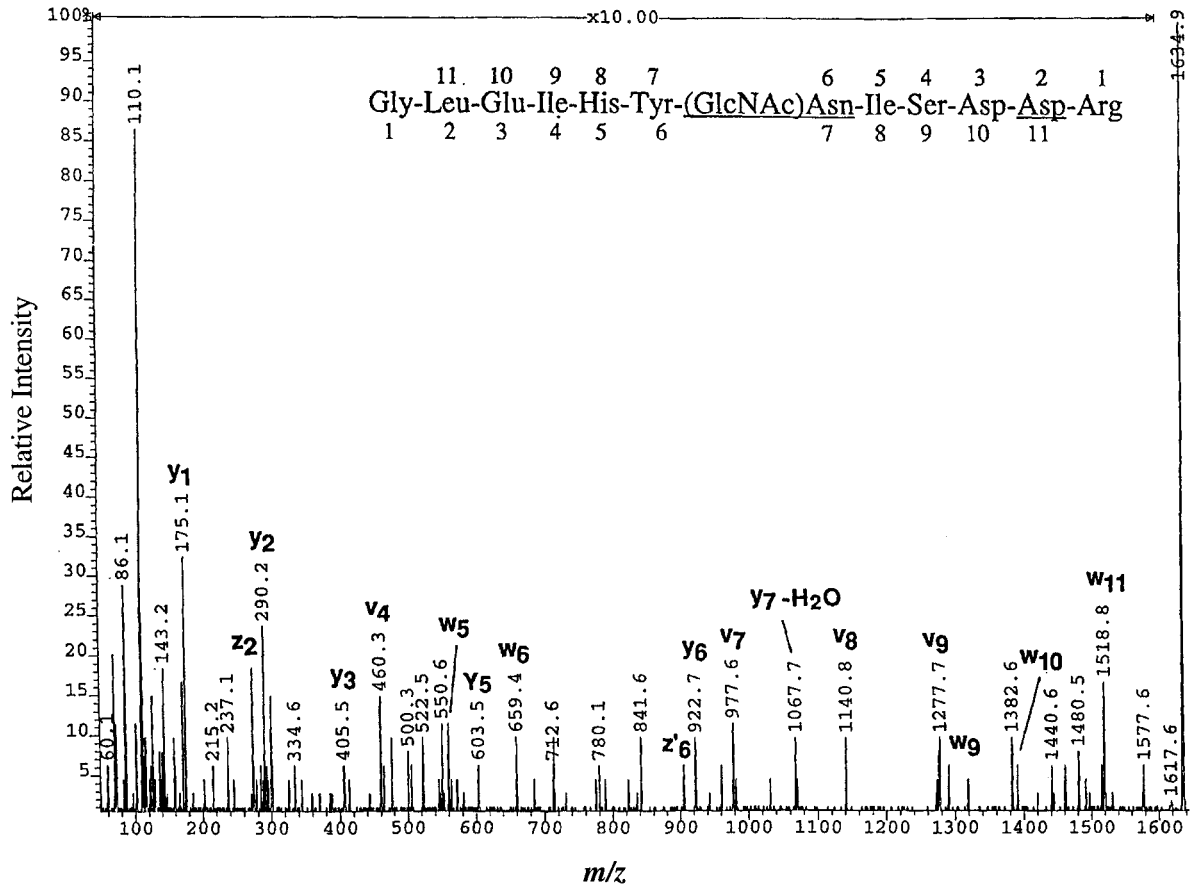


FIGURE 5: MALDI/CID spectrum of GP2,3 after sequential treatment with Endo H and PNGase F. GP2,3 (20 pmol) was treated with Endo H followed by PNGase F as described in Materials and Methods, and ~10 pmol of digest was analyzed by MALDI/CID in the posiitve ionization mode. The matrix used was 2,5-dihydroxybenzoic acid.

shown that the class of oligosaccharides at individual sites are overwhelmingly either oligomannosidic/hybrid or lactosamine-type. Interestingly, at Asn[193], both lactosamine-type and oligomannosidic structures were observed. Except for the case of the E1 glycoprotein of Sindbis virus (*21*), the presence of both classes of oligosaccharides at Asn[193] is the only other example suggesting "leakiness" in the pathway which converts oligomannose to lactosamine-type structures at an individual glycosylation site.

The absence of $Man_9GlcNAc_2$, the apparently small amount of $Man_5GlcNAc_2$ at Asn[99] and Asn[193], and the evidence for a single $Man_8GlcNAc_2$ isomer (*12*) suggest a limited processing pathway for the oligomannosidic structures. The removal of α(1→2)-linked Man residues in the ER is mediated by at least two α-mannosidases (*24*−*28*), which converts $Man_9GlcNAc_2$ to $Man_{6-8}GlcNAc_2$ oligosaccharides. An ER α-mannosidase, which is sensitive to the alkaloid kifunensine (ER mannosidase I), initially removes the middle-branch α(1→2)-linked Man residue while ER mannosidase II removes the Man residue from the upper branch α(1→6) side of the oligosaccharides (*28*). A single $Man_8$ isomer (*12*) and the removal of Man residues restricted to three residues is consistent with exoglycosidase processing at Asn[99] and Asn[193] occurring primarily in the ER without involvement of Golgi mannosidases.

The H,K-ATPase is a membrane-bound protein, a feature putatively associated with the addition of polylactosamine chains (*29*−*32*). However, it is now clear that polylactosamine structures are also present on secretory glycoproteins (*33*, *34*). Asparagine residues 130, 146, and 161 of the H,K-ATPase contains polylactosamine structures. The transferase which initiates polylactosamine synthesis, UDP-GlcNAc:Galβ1→4GlcNAc-R β1→3-*N*-acetylglucosaminyltransferase, has been shown to prefer a Galβ1→4GlcNAcβ1→2(Galβ1→4GlcNAcβ1→6)Man structure as a substrate (*35*), and most described glycoproteins with polylactosamine structures contain 2,6-disubstituted mannose residues within tri- and tetraantennary oligosaccharides (*30*). A recognized exception are the biantennary polylactosamine structures from the band 3 glycoprotein of erythrocytes (*36*), and it has been suggested that erythrocytes may have a different polylactosamine extension enzyme (*30*). The finding of biantennary oligosaccharides with up to two repeats at Asn[146] and Asn[161] indicates that the gastric parietal cell also contains a polylactosamine-initiating enzyme that does not require a Galβ1→4GlcNAcβ1→2(Galβ1→4GlcNAcβ1→6)Man unit for significant activity.

We found that the lactosamine-type oligosaccharides of the H,K-ATPase were completely terminated with α-linked Gal residues, the first report of an individual glycoprotein containing a singular neutral structure as the terminus. The individual branches of lactosamine-type chains of glycoproteins are usually terminated in sialic acid or α-linked Gal residues, both within the same structure (*38*−*43*). Further, the complete absence of sialic acid on a glycoprotein is unusual and all tissues examined in human and rat express at least one sialyltransferase (*44*), although in this study gastric tissue was not reported to have been analyzed. The α-galactosyl transferase from thyroid preferentially adds the Gal residue to the Man α(1,6) arm of oligosaccharides, which

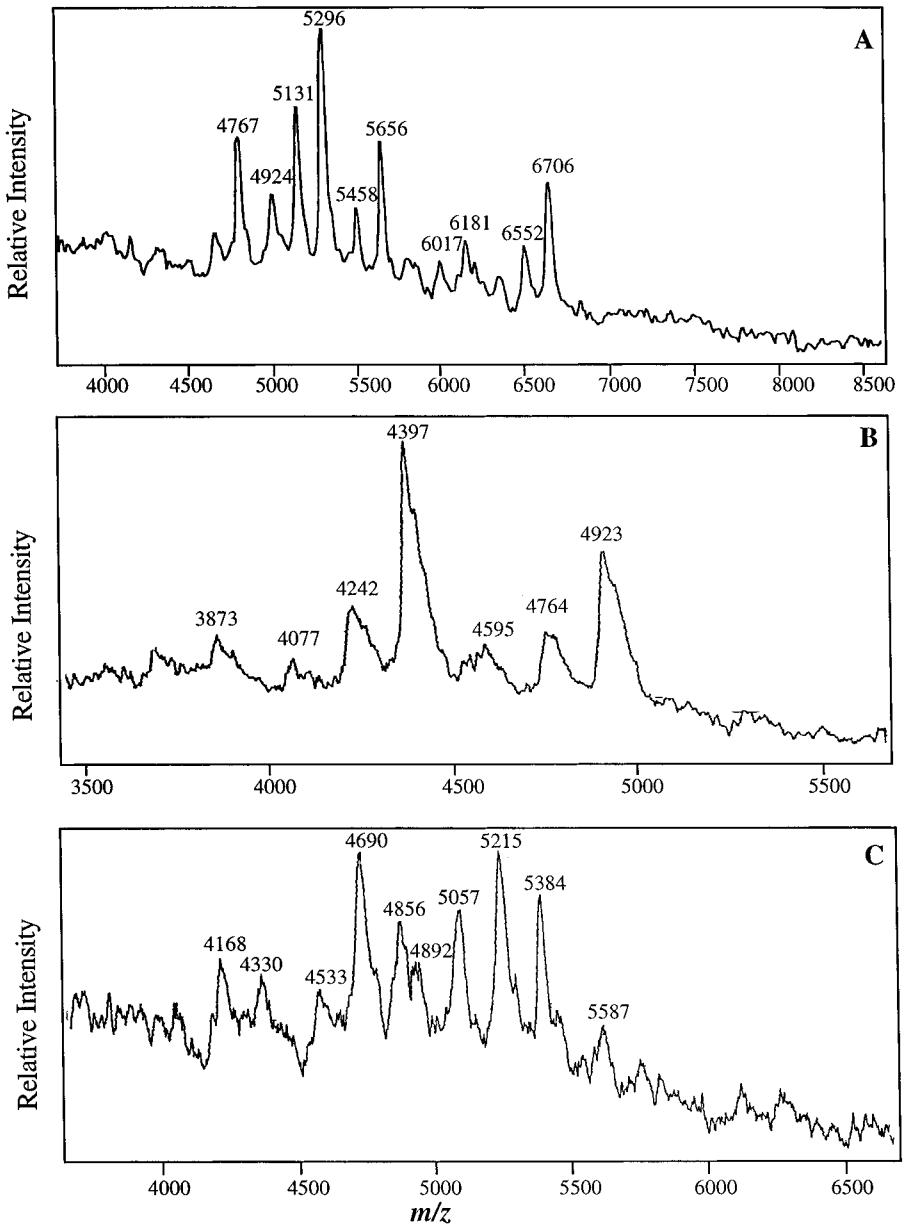


FIGURE 6: MALDI/MS of tryptic glycopeptides GP4, GP5, and GP6 of the $\beta$-subunit. Each spectrum was obtained using ~2 pmol of glycopeptide and the sum of ~25 laser shots. The matrix was α-cyano-4-hydroxycinnamic acid. (A) GP4 in the negative ionization mode; (B) GP5 in the positive ionization mode; (C) GP6 in the negative ionization mode.

complements the activity of sialyltransferases (*45*). The results, herein, show that the α-galactosyl transferase(s) in rabbit parietal cells efficiently transfers Gal to all branches of bi-, tri-, and tetraantennary structures. Whether the rabbit gastric parietal cells contain sialyltransferase activities will require further studies.

An unusual observation was the presence of oligosaccharides containing multiple α-linked Gal residues on linear polylactosamine branches. The only site having tetraantennary oligosaccharides ($Asn^{130}$) contained most of the "additional" α-linked Hex residues and a minor proportion of these structures were observed at $Asn^{146}$ and $Asn^{161}$. The studies, herein, showed that up to six Hex residues were lost from tetraantennary oligosaccharides after treatment with α-galactosidase. Glycopeptides from Ehrlich ascites tumor cells have been reported to contain Galα1→3(Galα1→6)-Gal units as the termini of polylactosamine structures (*46*) but a subsequent report disputed the presence of α(1→6)-linked Gal in Ehrlich ascites cells (*47*). This is the first report of oligosaccharides from "normal cells" with multiple α-Gal residues. However, it is noted that the evidence for multiple α-Gal residues on gastric $\beta$-subunit oligosaccharides comes exclusively from the mass data coupled with α-galactosidase treatment, thus, further studies will be needed to establish the linkage, the branch location, and the specific α-galactosyltransferase responsible for the addition of these multiple α-Gal residues.

Preliminary studies on the gastric $\beta$-subunit from other species indicate that the feature of non-sialylation is conserved through different species (*9*−*11*). Recent studies also suggest the presence of branch fucosylation on mouse and human gastric $\beta$-subunit (*48*) and the presence of α-Gal residues on cow and frog $\beta$-subunits (*49*). Thus, the lack of sialylation and the presence of alternative acid-stable chain-terminating residues appears to be a common motif of glycosylation of the gastric $\beta$-subunit. It is interesting in this context that the oligosaccharides of the closely related $\beta$-subunit of Na,K-ATPase are sialylated, thus non-sialylation

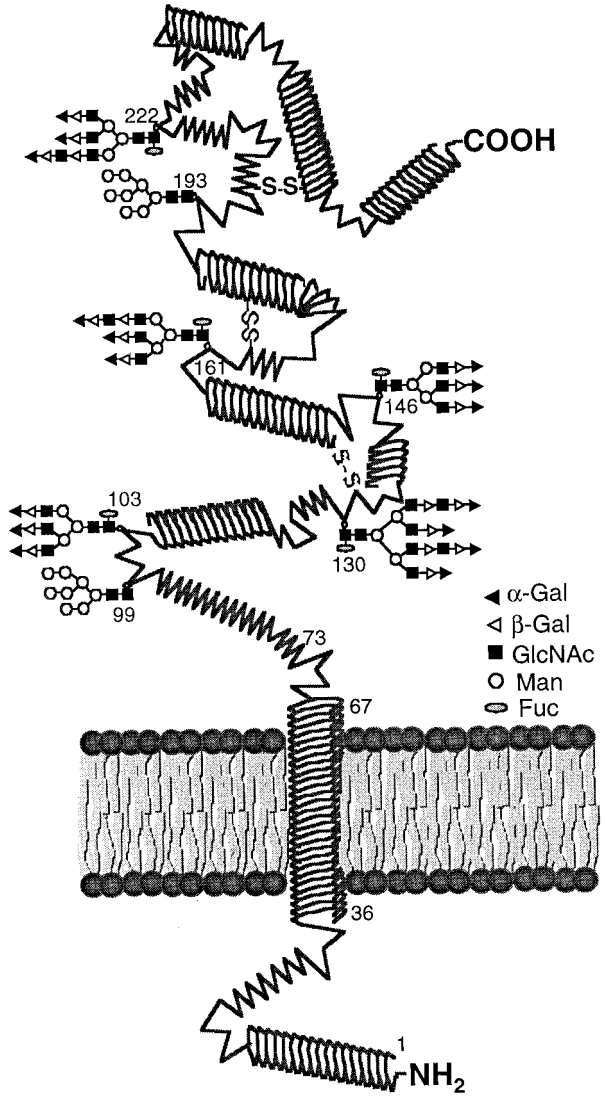


FIGURE 7: The $\beta$-subunit of the gastric H,K-ATPase.

is not a characteristic of P-type ATPases. Determination of whether the lack of sialylation and alternative end-terminal groups is essential for proton pumping function or is necessary for the survival of the enzyme in the harsh gastric environment requires further studies.

## ACKNOWLEDGMENT

The authors acknowledge Dr. David Maltby for obtaining the MALDI/CID spectrum and Dr. Katalina Medzihradszky for helpful discussions. The mass spectra were obtained at the UCSF Mass Spectrometry Facility supported by the Biomedical Research Technology Program of the National Center for Research Resources. The VG TofSpec SE was partially supported by Micromass, Beverley, MA. The VG AutoSpec was purchased with NIH NCRR BRTP RR01614 and NSF DIR 8700766.

## REFERENCES

1. Chow, D. C., Browning, C. M., and Forte, J. G. (1992) *Am. J. Physiol. 263*, C39−C46.
2. Tyagarajan, K., Chow, D. C., and Forte, J. G. (1995) *Biochim. Biophys. Acta. 1236*, 105−113.
3. Canfield, V. A., Okamato, C. T., Chow, D. C., Dorfman, J., Gros, P., Forte, J. G., and Levenson, R. (1990) *J. Biol. Chem. 265*, 19878−19884.
4. Reuben, M. A., Lasater, L. S., and Sachs, G. (1990) *Proc. Natl. Acad. Sci. U.S.A. 87*, 6767−6781.
5. Shull, G. E. (1990) *J. Biol. Chem. 265*, 12123−12126.
6. Toh, B. H., Gleeson, P. A., Simpson, R. J., Moritz, R. L., Callaghan, J. M., Goldkorn, I., Jones, C. M., Martinelli, T. M., Mu, F. T., Humphris, D. C., Pettitt, J. M., Mori, Y., Masuda, T., Sobieszczuk, P., Weinstock, J., Mantamadiotis, T., and Baldwin, G. (1990) *Proc. Natl. Acad. Sci. U.S.A. 87*, 6418−22.
7. Chow, D. C., Boyd, K. L., Scalley, M. L., and Forte, J. G. (1994) *FASEB J. 8*, A387, 2240.
8. Chow, D. C., Ushigome, M. M., Crothers, J. M. Jr., and Forte, J. G. (1993) *Gastroenterology 104*, A55.
9. Callaghan, J. M., Toh, B. H., Pettitt, J. M., Humphris, D. C., and Gleeson, P. A. (1990) *J. Cell Sci. 95*, 563−576.
10. Beesley, R. C., and Forte, J. G. (1974) *Biochim. Biophys. Acta 356*, 144−155.
11. Weitzhandler, M., Kadlecek, D., Avdalovic, N., Forte, J. G., Chow, D. C., and Townsend, R. R. (1993) *J. Biol. Chem. 268*, 5121−5130.
12. Tyagarajan, K., Townsend, R. R., and Forte, J. G. (1996) *Biochemistry 35*, 3238−3246.
13. Goldkorn, I., Gleeson, P. A., and Toh, B. H. (1989) *J. Biol. Chem. 264*, 18768−74.
14. Callaghan, J. M., Khan, M. A., Alderuccio, F., Van-Driel, I. R., Gleeson, P. A., and Toh, B. H. (1993) *Autoimmunity 16*, 289−295.
15. Reenstra, W. W., and Forte, J. G. (1990) *Methods Enzymol. 192*, 151−165.
16. Okamoto, C. T., Karpilow, J. M., Smolka, A., and Forte J. G. (1990) *Biochim. Biophys. Acta 1037*, 360−72.
17. Plummer, T. H., Jr., Phelan, A. W., and Tarentino, A. L. (1987) *Eur. J. Biochem. 163*, 167−73.
18. Bigge C., Patel, T. P., Bruce, J. A., Goulding, P. N., Charles, S. N., and Parekh, R. B. (1995) *Anal. Biochem. 230*, 229−238.
19. Hardy, M. R., and Townsend, R. R. (1994) *Methods Enzymol. 230*, 208−25.
20. Medzihradszky, K. F., Maltby, D. A., Qiu, Y., Yu, Z., Hall, S. C., Chen, Y., and Burlingame, A. L. (1997) *Int. J. Mass Spectrom. Ion Processes 160*, 357−369.
21. Hsieh, P., Rosner, M. R., and Robbins, P. (1983) *J. Biol. Chem. 258*, 2548−2554.
22. Hubbard, S. C. (1988) *J. Biol. Chem. 263*, 19303−19317.
23. Yet, M.-G., and Wold, F. (1990) *Arch. Biochem. Biophys. 278*, 356−364.
24. Bischoff, J., and Kornfeld, R.(1983) *J. Biol. Chem. 258*, 7907−7910.
25. Bischoff, J., Liscum, L., and Kornfeld, R. (1986) *J. Biol.Chem. 261*, 4766−4774.
26. Kabcenell, A. K., and Atkinson, P. H. (1985) *J. Cell Biol. 101*, 1270−1280.
27. Weng, S., and Spiro, R. G. (1996) *Arch. Biochem. Biophys. 325*, 113−123.
28. Weng, S., and Spiro, R. G. (1993) *J. Biol. Chem. 268*, 25656−63.
29. Fukuda, M., Guan, J. L., and Rose, J. K. (1988) *J. Biol. Chem. 263*, 5314−5318.
30. Do, K. Y., and Cummings, R. D. (1993) *J. Biol. Chem. 268*, 22028−22035.
31. van Hoek, A. N., Wiener,M. C., Verbavatz, J. M., Brown, D., Lipniunas, P. H, Townsend, R. R., and Verkman, A. S. (1995) *Biochemistry 34*, 2212−2219.
32. Treuheit, M. J., Costello, C. E., and Kirley, T. L. (1993) *J. Biol. Chem. 268*, 13914−13919.
33. Hokke, C. H., Bergwerff, A. A.,Van Dedem, G. W., Kamerling, J. P., and Vliegenthart, J. F. (1995) *Eur. J. Biochem. 228*, 981−1008.
34. Bloom, J. W.; Madanat, M. S., and Ray, M. K. (1996) *Biochemistry 35*, 1856−1864.
35. van den Eijnden, D. H., Koenderman, A. H., and Schiphorst, W. E. (1988) *J. Biol. Chem. 263*, 12461−12471.
36. Fukuda, M., Dell, A., Oates, J. E., and Fukuda, M. N. (1984) *J. Biol. Chem. 259*, 8260−8273.

37. Dorland, L., van Halbeek, H., and Vliegenthart, J. F. G. (1984) *Biochem. Biophys. Res. Commun. 122*, 859−866.
38. Geyer, R., Geyer, H., Egge, H., Schott, H. H., and Stirm, S. (1984) *Eur. J. Biochem. 143*, 531−539.
39. Goulut-Chassaing, C., and Bourrillon, R. (1995) *Biochim. Biophys. Acta 1244*, 30−39.
40. Santer, U. V., DeSantis, R., Hard, K. J., van Kuik, J. A., Vliegenthart, J. F., Won, B., and Glick, M. C. (1989) *Eur. J. Biochem. 81*, 249−60.
41. Pfeiffer, G., Schmidt, M., Strube, K.-H., and Geyer, R. (1989) *Eur. J. Biochem. 186*, 273−286.
42. Waard, P. de, Koorevaar, A., Kamerling, J. P., and Vliegenthart, J. F. G. (1991) *J. Biol. Chem. 266*, 4237−4243.
43. Anderson, D. R., Atkinson, P. H., and Grimes, W. J. (1985) *Arch. Biochem. Biophys. 243*, 605−618.
44. Kitagawa, H., and Paulson, J. C. (1994) *J. Biol. Chem. 269*, 17872−17878.
45. Joziasse, D. H., Shaper, N. L., Salyer, L. S.,Van den Eijnden, D. H., van der Spoel, A. C., and Shaper, J. H. (1990) *Eur. J. Biochem. 191*, 75−83.
46. Eckhardt, A. E., and Goldstein, I. J. (1983) *Biochemistry* **22**, 5290−5297.
47. Kamada, Y., Muramatsu, H., Kawata, M., Takamizawa, H., and Muramatsu, T. (1988) *J. Biochem. 104*, 738−741.
48. Appelmelk, B. J., Simoons-Smit, I., Negrini, R., Moran, A. P., Aspinall, G. O., Forte, J. G., De Vries, T., Quan, H., Verboom, T., Maaskant, J. J., Ghiara, P., Kuipers, E. J., Bloemena, E., Tadema, T. M., Townsend, R. R., Tyagarajan, K., Crothers, J. M., Jr, Monteiro, M. A., and Savio, A. (1996) *Infect. Immun. 64*, 2031−2040.
49. Tyagarajan, K., Crothers, J. M., Jr., Mulvihill, S. J., Lipniunas, P., Townsend, R. R., and Forte, J. G. (1995) *Gastroenterology 108*, A247.

BI9706125